Chapter 5

Natural Convection Heat Transfer from a Rectangular Block Embedded in a Vertical Enclosure

Xiaohui Zhang

Additional information is available at the end of the chapter

http://dx.doi.org/10.5772/52666

1. Introduction

In many circumstances of practical concern, thermal sources are encapsulated into closed cavities containing a fluid, such as in the case of fuel tanks. In other applications it is the heat source itself which needs to be thermally controlled, such as in electronic packaging, passive cooling, space heating, nuclear design, and geophysics; another example is the natural convection around a horizontally-placed or vertically-positioned radiator, which can be used for a centralized heating and cooling system to regulate the air temperature in a cavity. The location of the radiator affects the temperature distribution and heat transfer in a cavity. Normally, a higher position of the radiator is reasonable when the radiator is used as a cooling device, while a lower position for the radiator is reasonable when the radiator is used for a heating one. It is worth studying the temperature distribution and heat transfer in thermal management and design. Whether the radiator is used as a cooling device or a heating device, the heat transfer of a object in a cavity can be simplified and dominated by natural convection heat transfer mechanism in an enclosure with an isolated plate.

Shyy and Rao [1] conducted an investigation of transient natural convection around an enclosed vertical plate. Numerical simulations and experimental data of natural convection air cooling of an array of two-dimensional discrete flush heaters on a vertical wall of a rectangular enclosure were performed by Ho and Chang [2]. Yang and Tao [3] developed a computational method to deal with the internal isolated islands (set the main diagonal element coefficient big values in velocity discrete equations)for natural convection in an enclosure. Experimental work and numerical simulation were studied by Wang [4] regarding natural convection in an inclined cube enclosure with multiple internal isolated plates. Also, numerical analysis on a 3×3 array of discrete heat sources flush-mounted on one vertical wall of a rectangular enclosure filled with various liquids was done by Tou and

Tso [5]. Natural convection from a discrete bottom flush-mounted rectangular heat source on bottom of a horizontal enclosure was studied by Sezai and Mohamad [6]. Deng et al. [7] investigated numerically the steady state natural convection induced by multiple discrete heat sources (DHSs) in horizontal enclosures. Unsteady convection numerical modelling in a vertical channel with a square cylinder was studied by Saha [8], Static bifurcation was found by Liu and Tao [9,10] who performed numerical computations for the heat transfer and fluid flow characteristics of an internal vertical channel composed by a pair of parallel plates situated in an enclosure. Barozzi and Corticelli [11,12] investigated the two-dimensional buoyant flow in a closed cabinet containing two vertical heating plates with a time-accurate finite method. The predictions showed the long-term behavior of numerical solution is time-dependent. The studies mentioned above have not been concerned with the effect of location for heat source or heat sink on the fluid flow and heat transfer.

Following the pioneering numerical works mentioned above, the present study represents a further effort to extend the studies with numerical simulation. The main objective of this study is to analyze the variation effect of the horizontal and vertical location ratios, a/H and b/H, respectively (defined in the following section) for different cold and hot isolated vertical plates in an enclosure, with respect to the flow configuration, temperature distribution, temperature difference distribution (defined in the following section) and heat transfer characteristics of the natural convection. Effect of Rayleigh number on the fluid flow and heat transfer is also presented.

2. Physical model and numerical method

The physical configuration and boundary conditions of problems investigated in this study are shown in Fig. 1. The two horizontal walls are considered to be insulated, and the two vertical walls which have the same temperatures, as well as the isolated vertical plate are maintained at T_1 and T_2, respectively. In this study, the investigations are carried out through the variation of horizontal location ratio a/H and vertical location ratio b/H in the cases of $T_1 > T_2$ (in this case $T_1 = T_h, T_2 = T_c$) and $T_1 < T_2$ (in this case $T_1 = T_c, T_2 = T_h$).

In the present model, the flow is simulated as a two dimensional phenomenon with the following assumptions or simplifications: a) the fluid (air) is Newtonian, incompressible and the flow is laminar, and; b) the temperature difference $T_1 - T_2$ is small, so that the effect of temperature on fluid density is expressed adequately by the Boussinesq approximation. Next, we consider the following dimensionless variables:

$$X = \frac{x}{H}; Y = \frac{y}{H}; U = \frac{u}{U_R}; V = \frac{v}{U_R}; P = \frac{p}{\rho U_R^2}; \Theta = \frac{T - T_c}{T_h - T_c}; \mathrm{Pr} = \frac{\nu}{a}; Ra = \frac{g\beta H^3 \Delta T}{\nu a}.$$

where the reference velocity is defined as $U_R = (Ra\,\mathrm{Pr})^{1/2}\,\mathrm{a}/\mathrm{H}$.

The governing equations, that express the conservation of mass, momentum and energy in the fluid domain, become:

$$\frac{\partial U}{\partial X}+\frac{\partial V}{\partial Y}=0 \tag{1}$$

$$U\frac{\partial U}{\partial X}+V\frac{\partial U}{\partial Y}=-\frac{\partial P}{\partial X}+\frac{Pr}{(RaPr)^{1/2}}\cdot\nabla^2 U \tag{2}$$

$$U\frac{\partial V}{\partial X}+V\frac{\partial V}{\partial Y}=-\frac{\partial P}{\partial Y}+\frac{Pr}{(RaPr)^{1/2}}\cdot\nabla^2 V+\Theta \tag{3}$$

$$U\frac{\partial \Theta}{\partial X}+V\frac{\partial \Theta}{\partial Y}=\frac{K}{(RaPr)^{1/2}}\cdot\nabla^2\Theta \tag{4}$$

where $\nabla^2=\partial^2/\partial X^2+\partial^2/\partial Y^2$ and $K=k/k_f$, with k and k_f being the vertical block location conductivity and thermal conductivity of the fluid, respectively.

No-slip condition is imposed on all the walls for the velocities. Thermal boundary conditions are that $\partial\Theta/\partial Y=0$ for the horizontal insulated walls, and $\Theta=1$ for the inner heat source and $\Theta=0$ for the vertical cold walls or $\Theta=0$ for the inner heat sink and $\Theta=1$ for the vertical hot walls.

The average Nusselt number is given below:

$$Nu=\frac{\mathrm{H}}{2(\mathrm{H}+\mathrm{W})}\left(\int_0^{\mathrm{L/H}}-\frac{\partial T}{\partial X}\Big|_{X=0}dY+\int_0^{\mathrm{L/H}}\frac{\partial T}{\partial X}\Big|_{X=\mathrm{L/H}}dY\right) \tag{5}$$

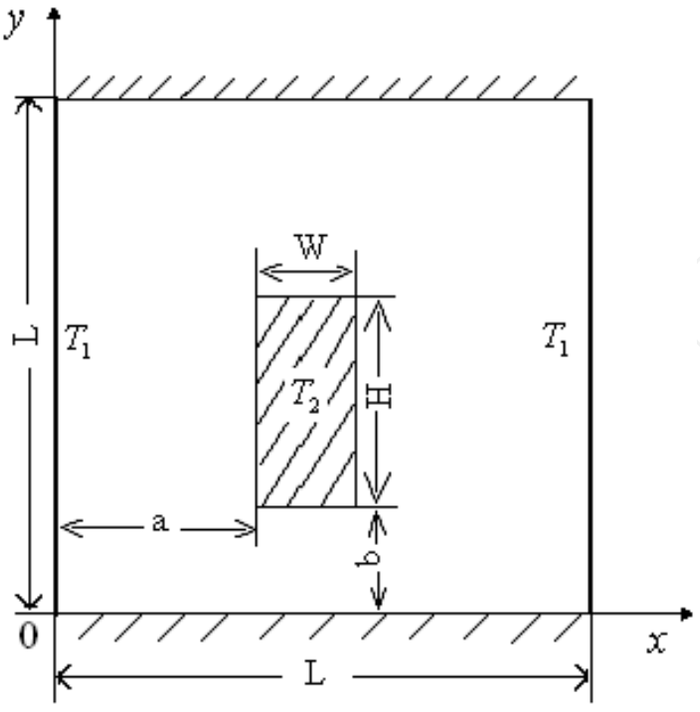

Figure 1. Schematic diagram of configuration

Equations (1) to (5) are solved using a finite volume method (FVM) on a staggered grid system [13]. In the course of discretization, QUICK scheme is adopted to deal with convection and diffusion terms. The equations from the discretization of Eqs. (1) to (4) are solved by the line-by-line procedure, combining the tri-diagonal matrix algorithm (TDMA) and successive over-relaxation iteration (SOR) and the Gauss-Seidel iteration technique with additional block-correction method for fast convergence. The SIMPLE algorithm [13] is used to treat the coupling of the momentum and energy equations. Pressure–correction and velocity-correction schemes are implemented in the model algorithm to arrive at converged solution when both the pressure and velocity satisfy the momentum and continuity equations. The solution is considered to converge when the sum of the normalized residuals for each control equation is of order 10^{-6} .

Special attention is paid to treatment of the isolated solid region. The presence of isolated area is accounted for by a strategy [3, 14] in which a part of solution domain is located in the flow field, therefore, the governing Eqs. (1) to (4) apply to both the fluid and the solid regions. Both the velocity and the dimensionless temperature in it remained zero in iteration process. For details, Ref.[3] may be consulted.

Non-uniform staggered grid system is employed with denser grids clustering near the plate and walls so as to resolve the boundary layer properly. Test runs are performed on a series of non-uniform grids to determine the grids size effects for the Rayleigh numbers 10^4, $10^5$and 10^6 at grid systems 40×40, 60×60 and 80×80, respectively. For each calculation case, a grid independent resolution is obtained. The maximum difference in average Nusselt number between grid (40×40) and grid (60×60) is 5%, the difference in average Nusselt number between grid (60×60) and grid (80×80) is less than 0.2%, so the 60×60 non-uniform grids are used.

The developed computational model is validated against benchmark computational results and is also compared with experimental data. Accuracy of the numerical procedure is validated by the comparison between the predicted results with the benchmark solutions of de Vahl Davis [15] for pure natural convection model in a square cavity with opposite heated and cooled side walls. As shown in Table 1, good agreements are achieved for both the maximum velocity and the average Nusselt number in a broad range of Rayleigh numbers Ra=10^4 to 10^6. Another comparison is also made with respect to the experimental work of Wang [4]. The computationally obtained flow patterns for $Ra=2\times10^5$ are compared with the flow visualization in Fig. 2. It is seen that the model adequately predicts the flow patterns obtained in the visualizations.

Ra	Present		Benchmark	
	$U_{\max}$	Nu	$U_{\max}$	Nu
10^4	0.192	2.231	0.193	2.245
10^5	0.129	4.50	0.132	4.510
10^6	0.078	8.817	0.077	8.806

Table 1. Comparisons between the predicted results and the benchmark resolutions of de Vahl Davis[15]

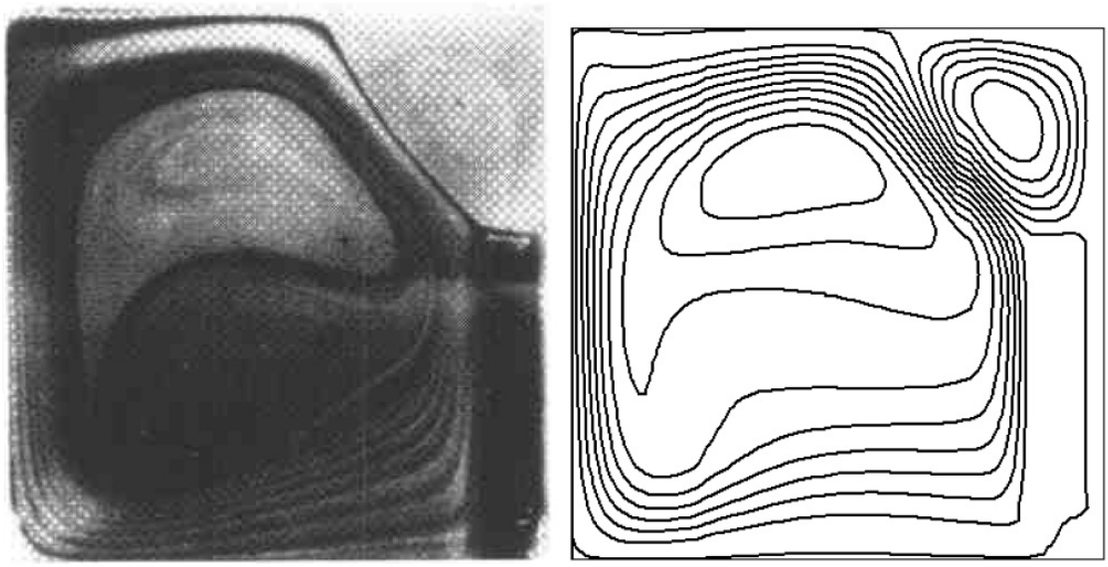

Figure 2. Flow field (a) Flow visualization [4], (b) Computation

3. Results and discussion

The configuration dimension is in the proportion of $L:H:W = 80:15:3$ .We will examine the fluid flow and heat transfer characteristics under the circumstances of heating or cooling at various locations, followed by the dependence to the Rayleigh number.

3.1. Effect of location on the fluid flow and heat transfer

Numerical simulations have been conducted to elucidate the effect of location ratios variation a/H $(0.3 \le a/H \le 2.7,\ b/H = 0.3)$ and b/H $(0.3 \le b/H \le 4.0,\ a/H = 0.3)$ on the natural convection of a cold isolated vertical plate and hot isolated vertical plate in an enclosure, Rayleigh number is fixed at $Ra = 2.5 \times 10^4$ in both cases.

3.2. Flow and temperature fields

The buoyancy-driven flow and temperature fields in the enclosure for a cold plate and a hot plate with the variation of location ratios a/H and b/H are illustrated by means of contour maps of streamlines and isotherms, respectively, as exemplified in Figs. 3 to 6.

For Fig.3 (a-f), there are two vortices flow where the directions are different for cold plate and hot plate. With the increase of horizontal location ratio a/H near the middle of the enclosure, the two vertices structure around the vertical plate tend to be more symmetric for cold plate and hot plate. The spaces at the two sides of the plate are large enough for the flow within it to develop, so buoyant convection flow is strong on the upper surface of hot plate, indicating the strong effect of the natural convection, while convection is weak in the case of cold plate relatively.

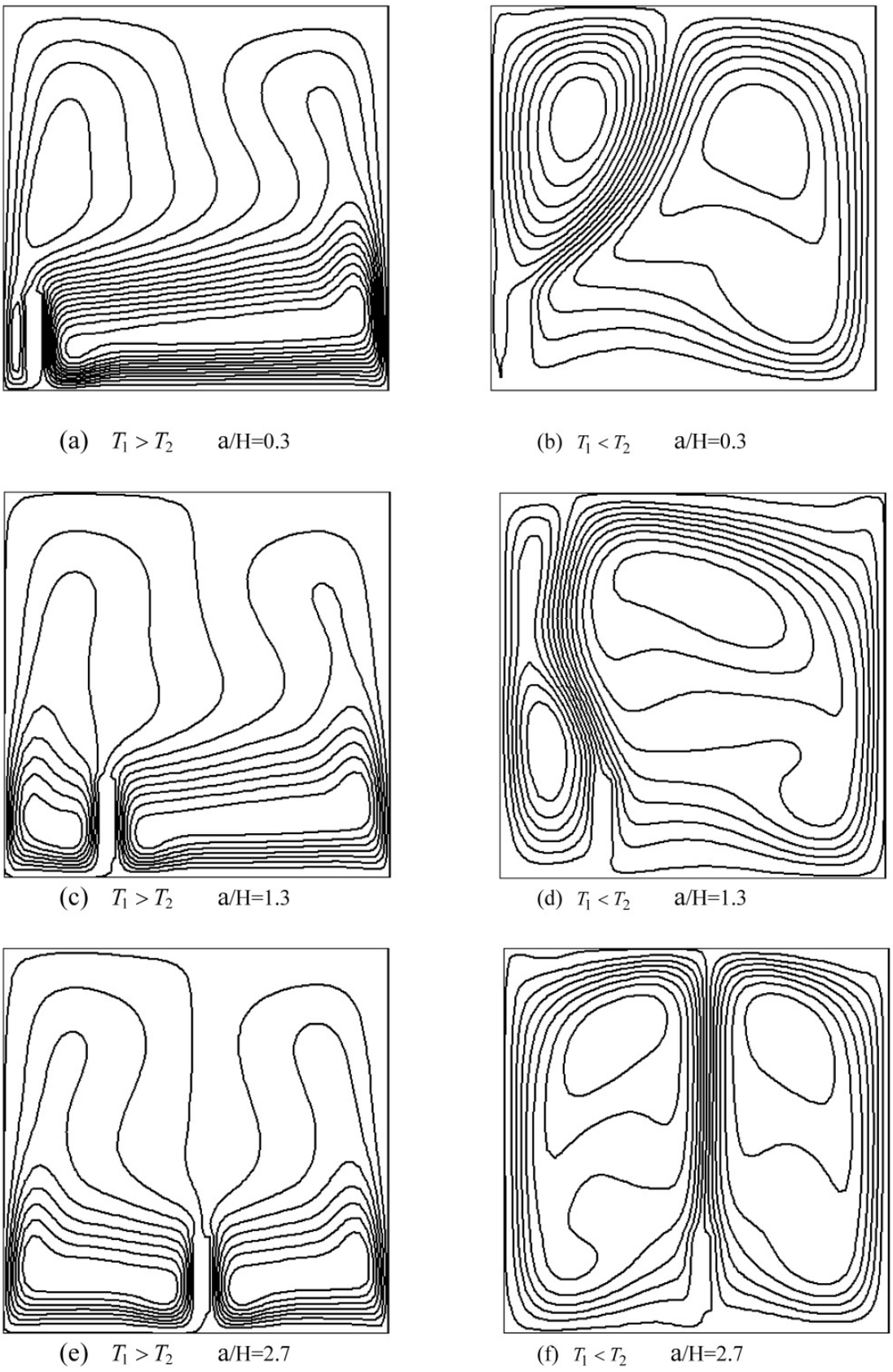

Figure 3. Streamlines for different horizontal locations at $Ra = 2.5 \times 10^4$

Dimensionless temperature distributions, plotted against the variation of the horizontal location ratio a/H , are displayed in Fig.4 (a-f). From this plot, it can be seen that isotherms near walls are almost vertical up to the upper and lower walls. This is due to the conduction effect. The figures reveal also that dimensionless temperature distributions of cold plate are more stratified than those of the hot plate.

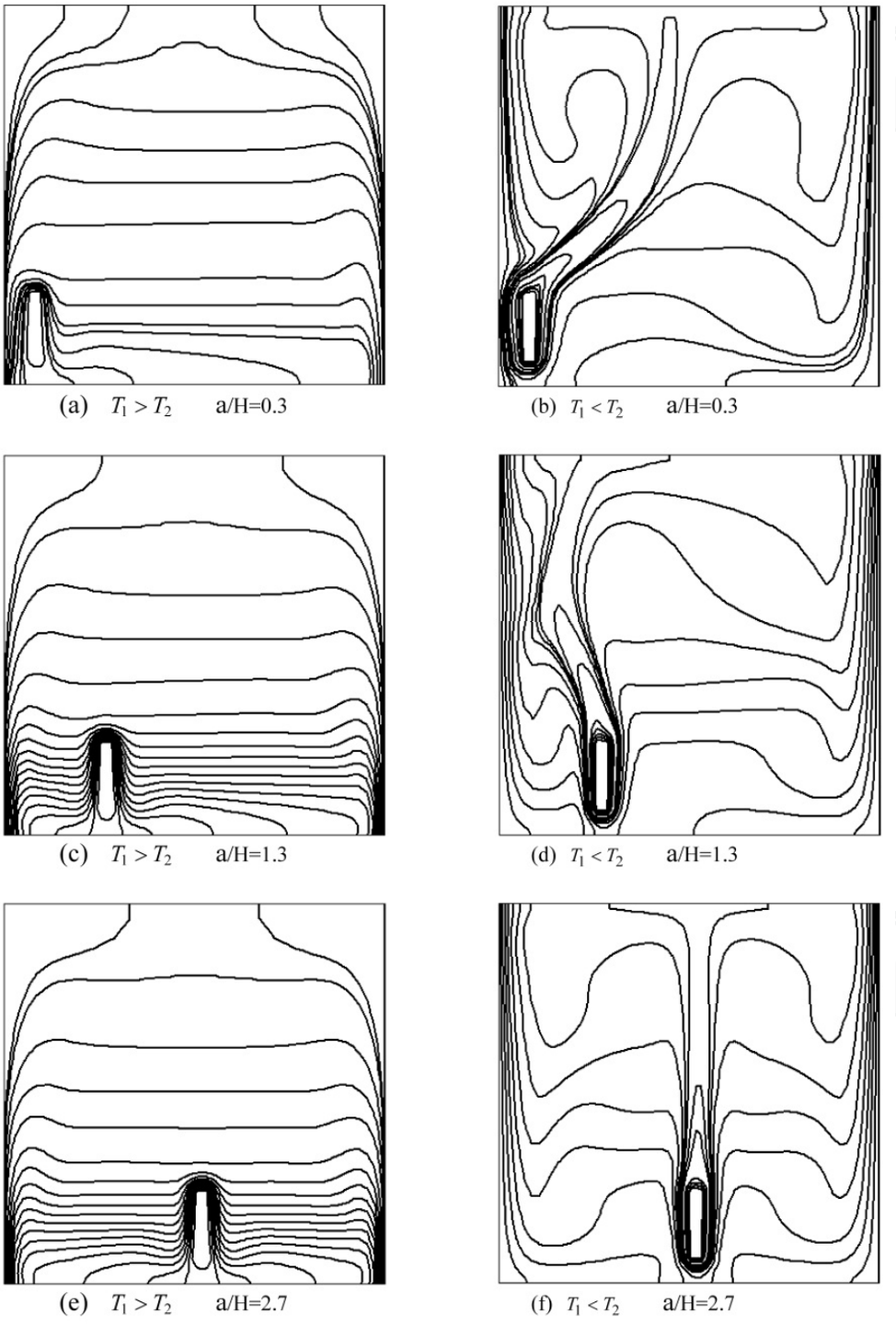

Figure 4. Isotherms for different horizontal locations at $Ra = 2.5 \times 10^4$

For Fig. 3(a and b), Fig. 5 and Fig. 6, we observe significantly different fluid flow and temperature distribution phenomena: the larger of the vertical location ratio b/H, the stronger the flow below the cold plate surface, and the more stratified temperature distribution for the hot plate.

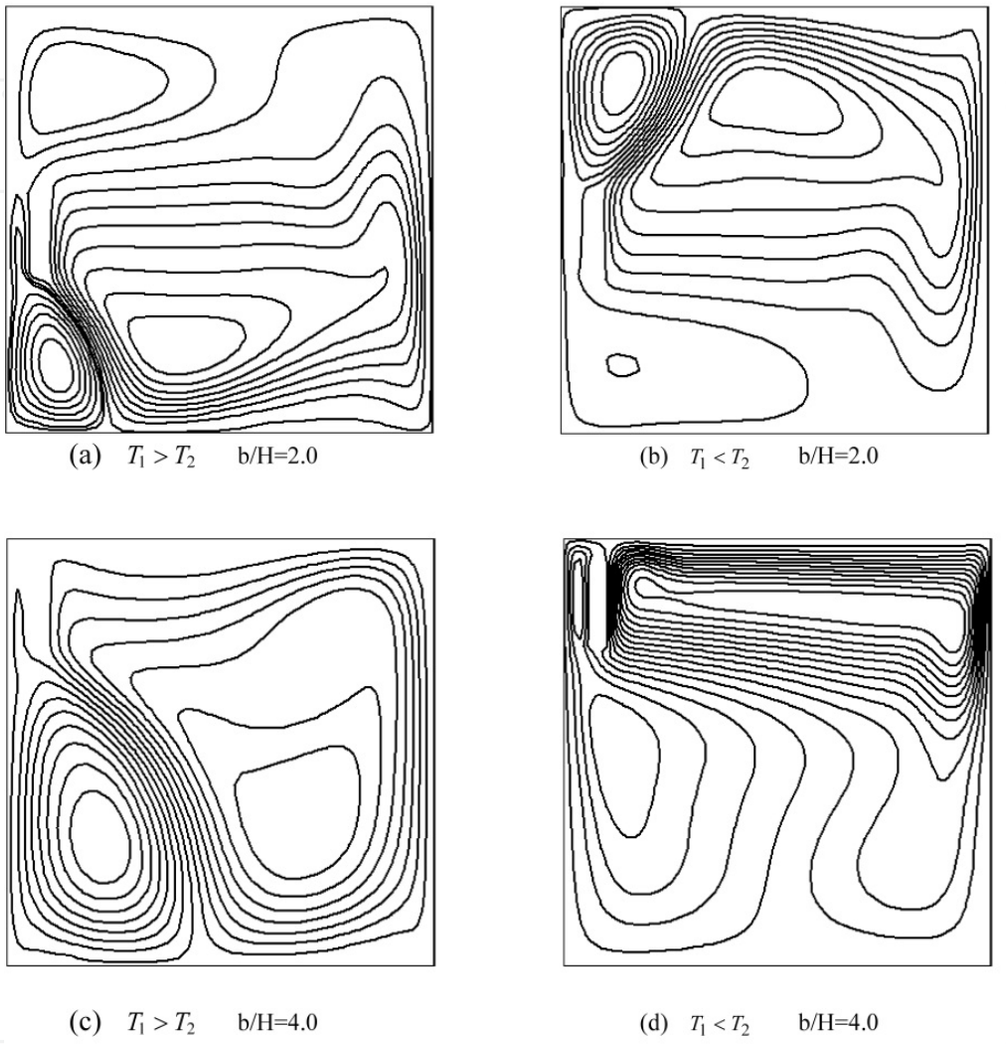

Figure 5. Streamlines for different vertical locations at $Ra = 2.5 \times 10^4$

It is apparent from the comparison of fluid flow configurations and dimensionless temperature distributions of the cold plate and hot plates that the vertical location ratio b/H has a substantial effect on the flow configuration and temperature profile.

3.3. Temperature difference distribution

Uniform temperature difference in an enclosure may have practical importance, particularly in electronics and air conditioning. In order to describe the uniformity of temperature difference in an enclosure we define TD, which means difference of node temperature and average temperature where average temperature is obtained by a weighted area method.

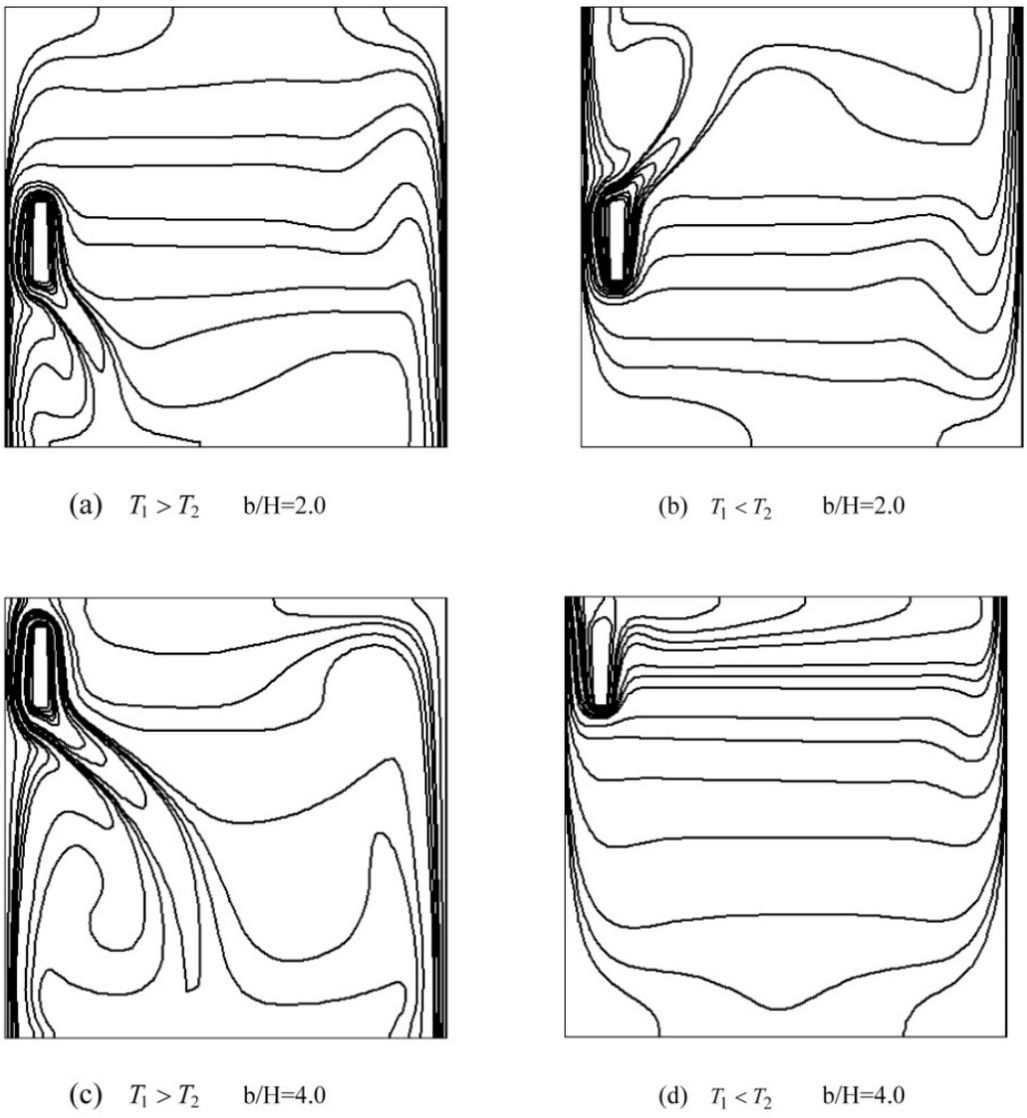

Figure 6. Isotherms for different vertical locations at $Ra = 2.5 \times 10^4$

$$\mathrm{TD} = t_{ij} - \frac{\sum t_{ij} A_{ij}}{\sum A_{ij}} \tag{6}$$

Two cases are studied at $Ra = 2.5 \times 10^4$, case 1: a/H =0.3 and b/H =0.3, and case2: a/H =0.3 and b/H =2.0. Figure 7 shows the temperature difference distribution, marked as TD and plotted against the height of enclosure, while the width is fixed for heating and cooling conditions.

It can be seen that, in case 1, the temperature difference of heating condition along the height of enclosure is more uniform (the maximum dimensionless temperature difference is 0.11) than that for cooling condition (the maximum dimensionless temperature difference is 0.48). While with the increase of height, the dimensionless temperature differences between heating condition (the maximum dimensionless temperature difference is 0.203) and cooling

condition (the maximum dimensionless temperature difference is 0.245) are not great along the height of enclosure in case 2. It implies that the requirement of heating and cooling in case 2 for same component can be met.

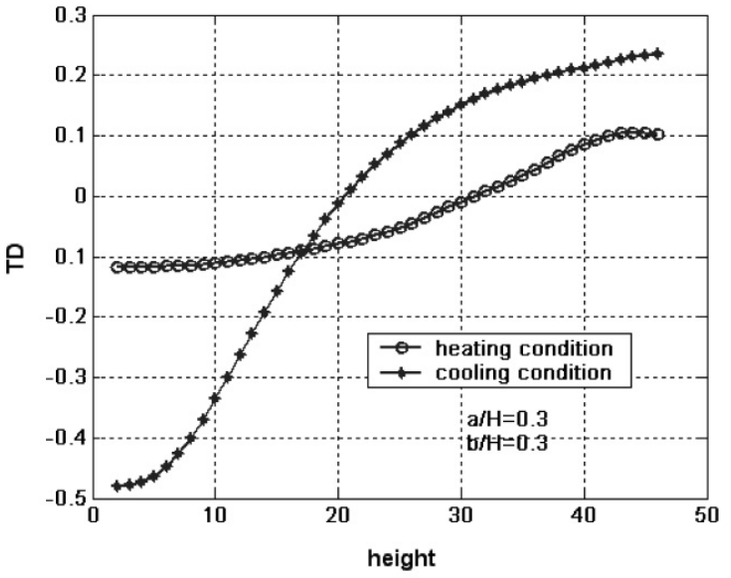

(a) case1

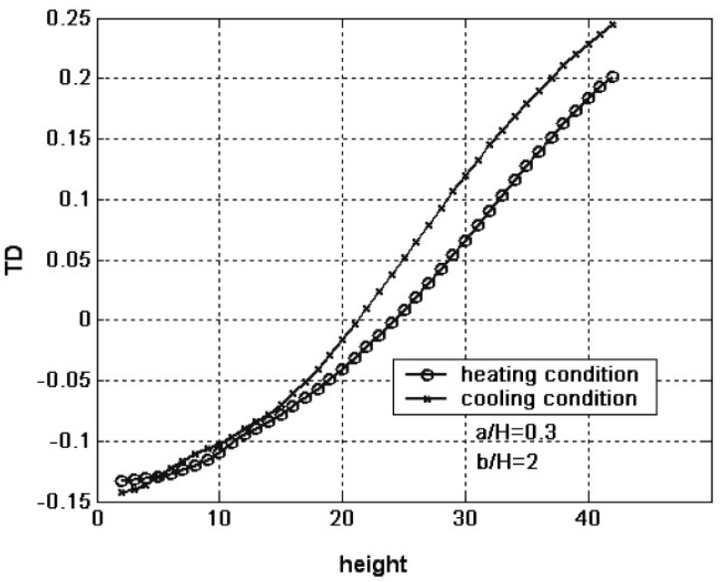

(b) case2

Figure 7. Variation of temperature difference with the height of enclosure for heating and cooling condition

3.4. Heat transfer

Next, attention is focused on the role which the location ratio can play in the heat transfer rate. Figures 8 and 9 present results of the average Nusselt number defined by Equation (5).

For both the cold and the hot plates, b/H is fixed at 0.3. Results show that the same trend occurs with the increase of a/H for both cold plate and hot plate. When the plate is within a wide range of enclosure values, 0.3< a/H <4.8, the effect of its location on heat transfer is small. The variation character of Nu vs. a/H implies that in a wide range of a/H , the spaces at the two sides of the plate are large enough for the flow within it to develop, therefore, the average heat transfer rate is not sensitive to the distance from the side wall. Indeed, the average hot plate Nusselt number is 20% to 39% higher as compared to that of the cold plate. The fact that the average Nusselt number of the hot plate is higher than the corresponding cold plate, can be explained if we consider the streamlines shown in Fig. 3 and temperature profiles in Fig. 4. From these figures we note that the natural convection occurs easier for the hot plate, due to a higher heat transfer than for the cold plate under the same boundary conditions. The steep increase of average Nusselt number near walls for the cold and hot plates in Fig. 8 is referred to as the "chimney effect". The present results confirm the fact that the stronger chimney effect enhances the heat transfer [16, 17]. For Pr ≈1, the boundary layer thickness for the plate scales as [18],

$$\delta = \delta_T \approx y\left(\frac{g\beta\Delta T y^3}{a\nu}\right)^{-1/4} \tag{7}$$

Which indicates that δ increases as $y^{1/4}$.

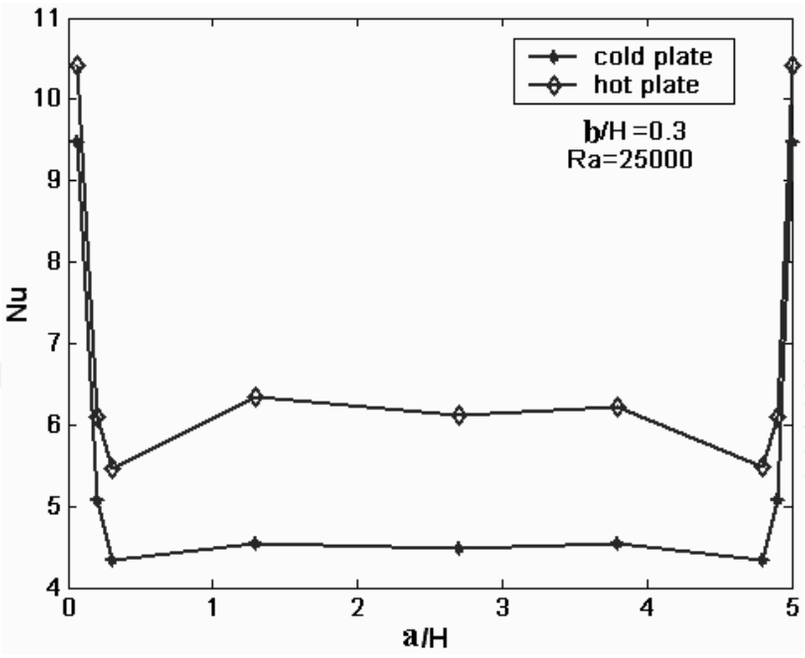

Figure 8. Variation of Nu with horizontal location

The convection is enhanced due to the instability of thermal boundary layers near the left plate and right wall (0< a/H <0.3) or right plate and left wall (4.8< a/H <5). In this spacing, the thermal boundary layers of wall and plate merge with each other, so the boundary layer

thickness is thin leading to the increase of Nusselt number. Therefore, the characteristics of the fluid flow and heat transfer in enclosure are very sensitive to the distance between the wall side and the plate.

Different trends occur when the cold plate and the hot plate are at different vertical location which is shown in Fig. 9. Study of Fig. 9 reveals that for cold plate, as the vertical location ratio increases from 0.3 to 3.3 the average Nusselt number increases from 4.33 to 5.68, and slightly decreases from 5.68 to 5.52 when location ratio increases to 4. That means there exists a maximum average Nusselt number when cold plate location $(b/H)_{opt}$ is 3.3. For the hot plate, average Nusselt number slightly increases from 5.47 to 5.61 when location ratio increase from 0.3 to1.33, and decreases from 5.61 to 4.3 when vertical location ratio increases from 1.33 to 4. There is an appropriate location which corresponds to a maximum heat transfer density for the hot plate also. This can be attributed to two different flow patterns. However, the average Nusselt number variation is not significant for cold and hot plates.

By comparison of Fig. 3(a and b), Fig. 5(c and d), Fig. 6(c and d), and Fig. 9, it can be seen that the symmetry phenomenon appears, *i.e.* the identical problems of natural convection in an enclosure [19].

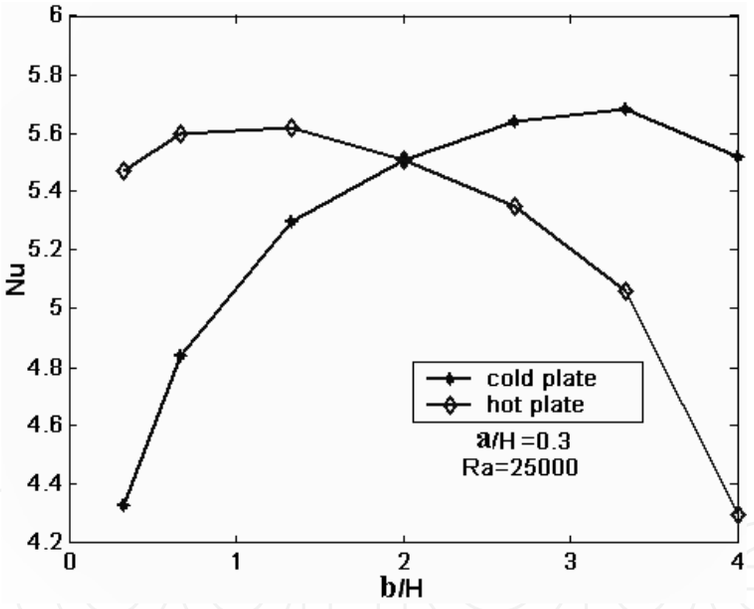

Figure 9. Variation of Nu with vertical location

3.5. Effect of Ra on the fluid flow and heat transfer

The procedure is then repeated over the range $10^2 \le Ra \le 10^8$. The effect of the Rayleigh number on the average Nusselt number by setting a/H =0.3 and b/H =0.3 under the circumstances of heating or cooling the block is shown in Fig. 10.

The flow patterns and isotherms are drawn for two typical Rayleigh numbers: $Ra = 1.0 \times 10^2$ and $Ra = 1.0 \times 10^7$ for one geometrical configuration a/H =0.3 and b/H =0.3. These are presented in Figs. 11 and 12.

For the low Rayleigh numbers (Ra=$10^2 - 10^4$), the flow field consists of a single big vortex in the half domain of cavity. With an increase in Rayleigh number, the heat transfer process is dominated successively by conduction mode, combined mode of conduction-convection and convection mechanism. When the Rayleigh number increases to as high as 1.0×10^7, it indicates the convection mode is predominated, these can be seen from Figs. 11 and 12.

At the lower Rayleigh numbers (Ra=$10^2 - 10^4$), Nusselt number of heating condition is a little bit higher than that of cooling condition which can be explained that convection of the hot plate is easier to establish than that of cold plate, conduction mechanism is prevailed and hence heat transfer is mainly dominated by conduction. That is why the Nu values shown in Fig. 10 are almost constant in the low Ra number range.

With the increase in Rayleigh number, Eq. (7) shows that at high Rayleigh numbers, the boundary layers on the enclosure right wall and plate left surface become very thin, leading to a significant increase in Nusselt number. It can be seen from Figs. 10 to 12 that in the convection regime ($Ra > 10^4$), the flow fields difference between the cold plate and the hot plate is appreciable, and the deviations of the Nusselt number between the cold plate and the hot plate are greater. The reason is that heat convection of the hot plate is easier to establish than that of the cold plate.

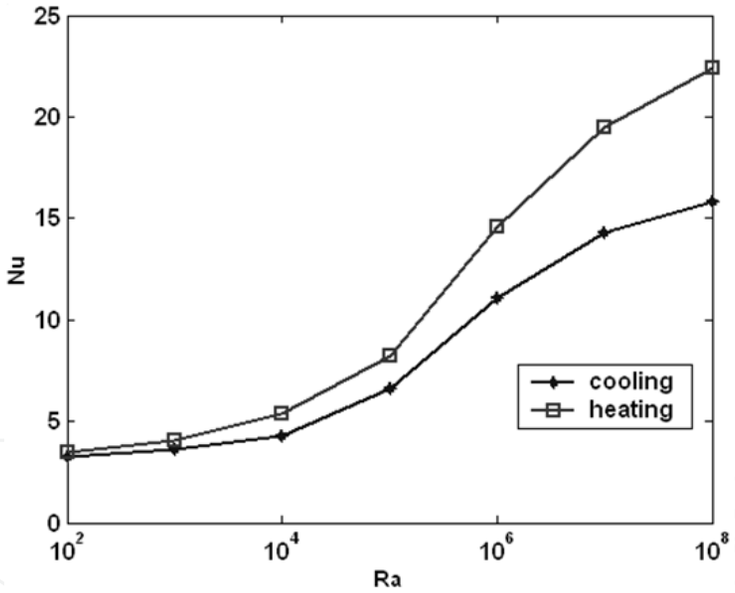

Figure 10. Nu versus Ra for heating and cooling cases

3.6. Special case -non steady state prediction

When the isolate is located in the middle of the enclosure,i.e. *L:H:W:b*=80:15:4:5, After giving definition of dimensionless time $F = \frac{a\tau}{H^2}(Ra\,\mathrm{Pr})^{\frac{1}{2}}$, it is easy get the dimensionless non-steady governing equation based on Equation(1)-(4).

The boundary conditions for this system are as same as steady system above.

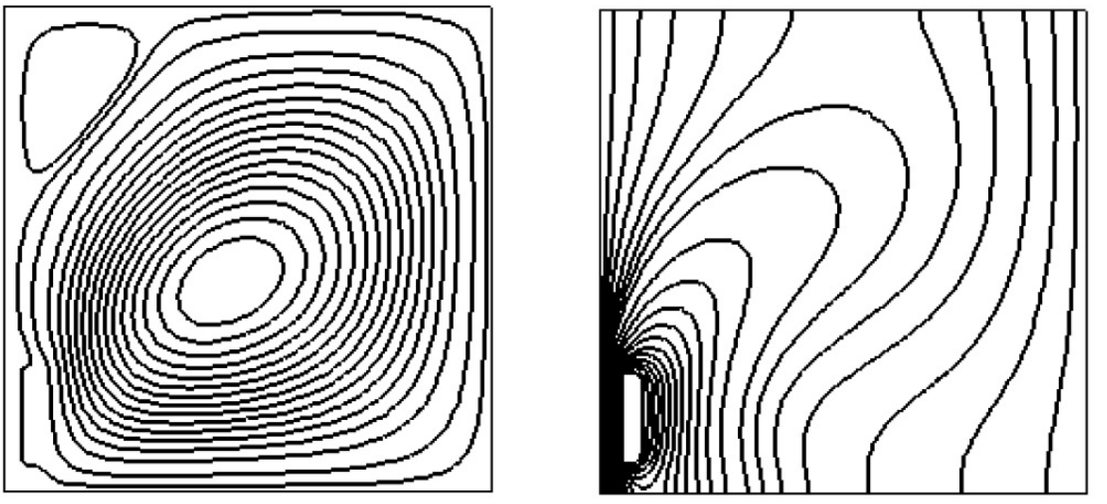

(a) $Ra = 1.0 \times 10^2$

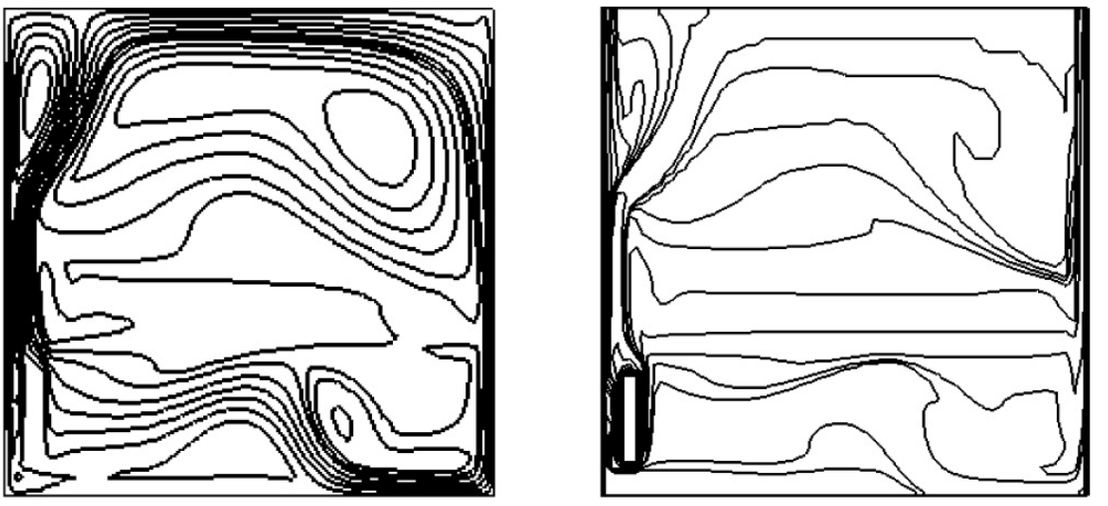

(b) $Ra = 1.0 \times 10^7$

Figure 11. $T_1 < T_2$ flow patterns (left) and isotherms (right) at different Rayleigh numbers

The zero initial conditions set for velocity and temperature fields.

A perfectly time-periodic solution is predicted shown in Fig. 13 for different Raleigh number(Ra=10^4, Ra=5x10^4, Ra=10^5 and Ra=10^6). Fig. 13a reports the time dependent behavior of dimensionless temperature at the monitoring point $(x, y) = (1.3, 1.53)$ of the cavity, and the average Nusselt number result is depicted in Fig. 13c. The first noteworthy feature of Fig. 13 is that, except low value of Ra number(Ra=10000,50000)，after a few time units, a transition to oscillatory flow occurs. the symmetric solution breaks down as instabilities grow, and the time behaviors of quantities relative to geometrically symmetric points begin to differ, The quantities at location $(x, y) = (1.3, 1.53)$ exhibit a clearly periodic behavior for Ra=100000(Fig. 13c,d), the period being about 10 time unit.

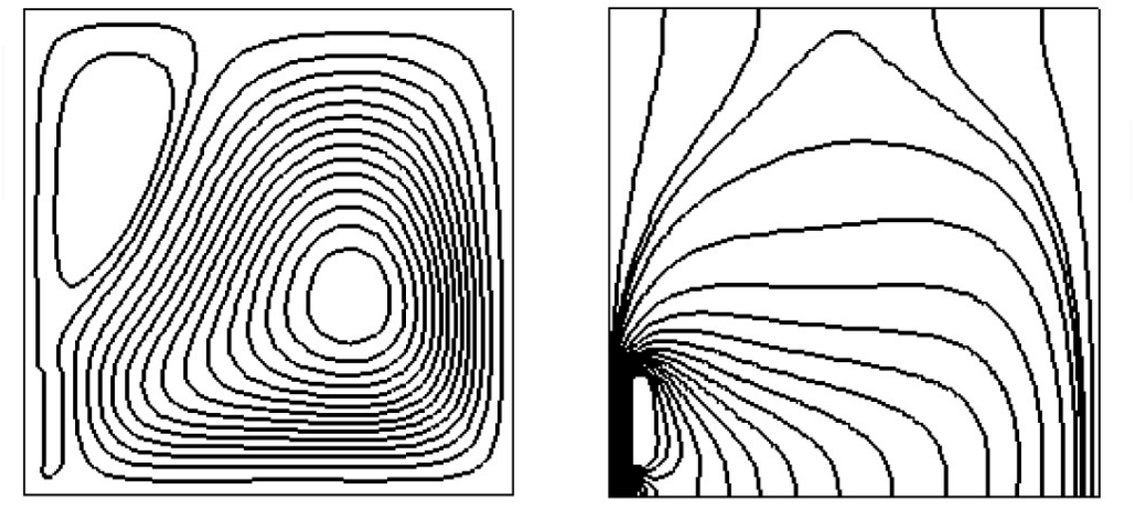

(a) $Ra = 1.0 \times 10^2$

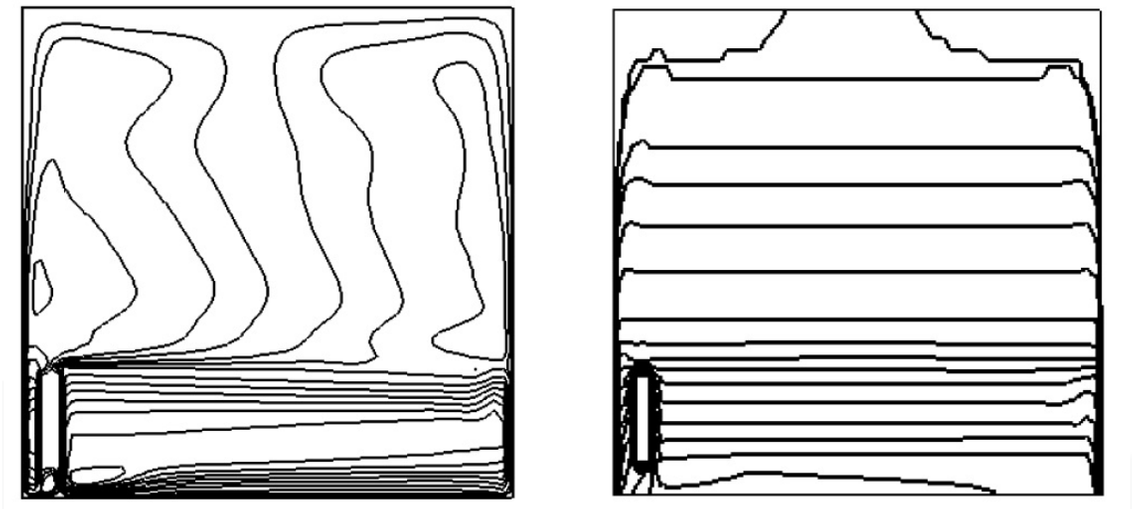

(b) $Ra = 1.0 \times 10^7$

Figure 12. $T_1 > T_2$ flow patterns (left) and isotherms (right) at different Rayleigh numbers

The isotherms are plotted in Fig. 14 for approximately equal time interval in one periodic circle When analyzing the macroscopic nature of the flow configurations, We observe the isotherms are not centrosymmetric at any point in time. The flow configurations manifest themselves in same pattern—the rolls movie to the left or right with the oscillation.

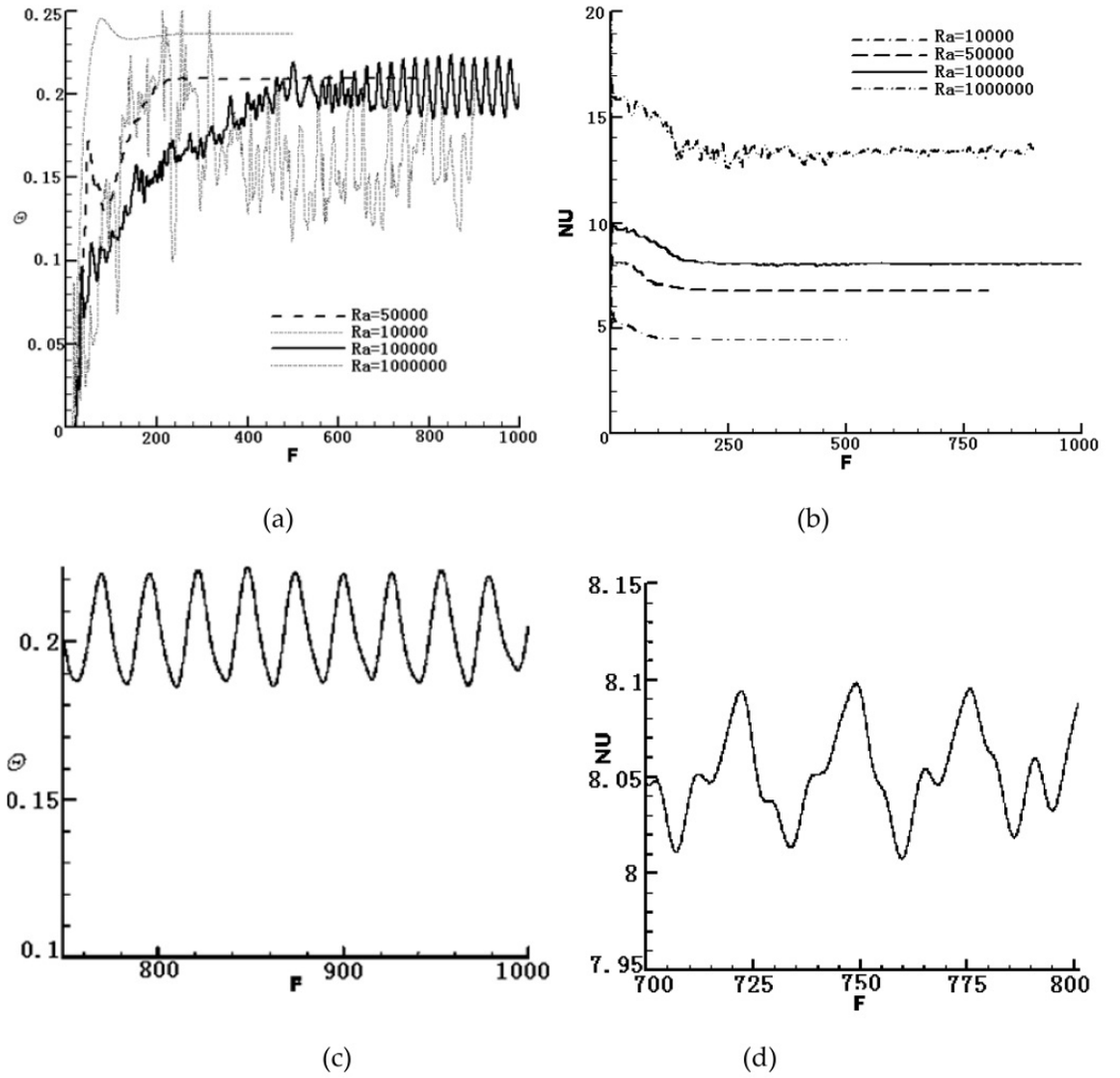

(a)variation of dimensionless temperature with dimensionless time for Ra=10000,50000,100000,1000000 at the monitoring point $(x, y) = (1.3, 1.53)$ of the cavity

(b) variation of average Nusselt number with dimensionless time for Ra=10000,50000,100000,1000000 at the monitoring point $(x, y) = (1.3, 1.53)$ of the cavity

(c) Partial enlargement of $T-F$ at the monitoring point $(x, y) = (1.3, 1.53)$ in the cavity for $Ra=10^5$

(d)Partial enlargement of $Nu-F$ at the monitoring point $(x, y) = (1.3, 1.53)$ in the cavity for $Ra=10^5$

Figure 13. Time history of the dimensionless temperature and Nusselt number at the monitoring point $(x, y) = (1.3, 1.53)$ of the cavity

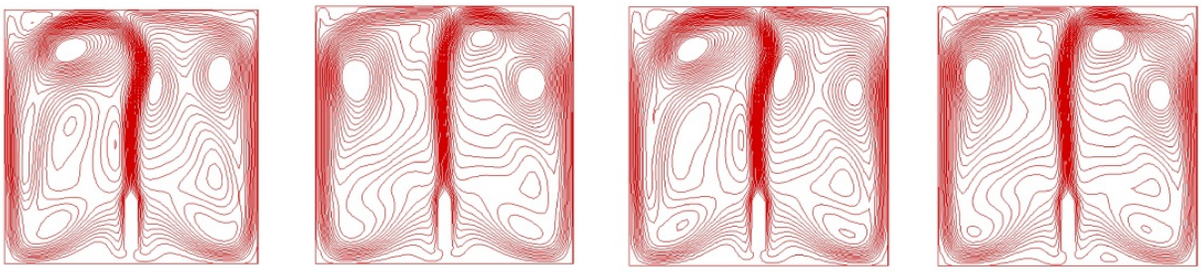

Figure 14. Series of instantaneous streamlines for Ra =10^5

4. Concluding remarks

A numerical study has been presented to unveil primarily the effect of location ratio variation of cold isolated vertical plate and hot isolated vertical plate on the natural convection in an enclosure. We conclude as follows from the numerical results.

a. The flow configurations and dimensionless temperature profiles of cold plate and hot plate are different;
b. The stratification is found to be strong for cold plate, while for the hot plate is relatively weak;
c. The temperature difference along the height of the enclosure in heating conditions is more uniform than that obtained in cooling conditions;
d. The increase of vertical location near the middle of enclosure leads to small temperature differences in heating and cooling conditions;
e. The trend of the average Nu number variation is the same for the cold and hot plates, when the plate is fixed at different horizontal locations. However, the average Nu number of the hot plate is about 20% to 39% larger than that of cold plate at the same Rayleigh number of 25000. For narrow distances between the inner plate and the bounding wall, the inner plate Nusselt number is enhanced, aside from this, the plate average Nusselt number is insensitive to the plate position;
f. The average Nu numbers tend to decrease with the increase of vertical location ratio ($1.33< b/H <4$) for hot plate, but for the cold plate the average Nu number tends to augment with the increase of vertical location ratio ($0.3< b/H <3.3$);
g. An optimum vertical location ratio exists at which the heat transfer is maximum for both cold and hot plates at a specific Rayleigh number;
h. Non-steady modeling simulations reveals that solutions are unique for values of Rayleigh number 10^4 and 5×10^4 where the flow and heat transfer is steady state. While unsteady state flow and heat transfer is appeared as a function of Ra=10^5 and Ra=10^6 for the rectangular block located in the middle of the cavity.

Nomenclature

a	horizontal location
A	node (i,j) based control volume area
b	vertical location
F	non-dimensional time
g	gravitational acceleration
H	height of vertical plate
k	vertical block location thermal conductivity
k_f	fluid thermal conductivity
K	relative thermal conductivity
L	characteristic length of the enclosure
Nu	Nusselt number
p	pressure
P	non-dimensional pressure
Pr	Prandtl number
Ra	Rayleigh number
t	node (i,j) temperature
T	temperature
TD	temperature difference
u,v	velocity components
U,V	dimensionless velocity
W	width of vertical plate
x,y	Cartesian coordinates
X,Y	dimensionless coordinates

Greek symbols

a	thermal diffusivity
β	coefficient of thermal expansion
δ	velocity boundary layer thickness
δ_T	thermal boundary layer thickness
ρ	density of the fluid
ν	kinematic viscosity of the fluid
Θ	dimensionless temperature

Subscipts

c	cold
h	hot
opt	optimization
R	reference

Author details

Xiaohui Zhang
School of Physical Science and Technology, School of Energy, Soochow University, Suzhou, China

Acknowledgement

This work is supported by National Natural Science Foundation of China（No.51176132）

5. References

[1] Shyy, W., and Rao, M.M., Simulation of Transient Natural Convection around an Enclosed Vertical Plate, *ASME J. Heat Transfer*, vol. 115, pp. 946–953, 1993.

[2] Ho, C.J., and Chang, J.Y., A Study of Natural Convection Heat Transfer in a Vertical Rectangular with Two-dimensional Discrete Heating: Effect of Aspect Ratio, *Int. J. Heat Mass Transfer*, vol. 37, pp. 917–926, 1994.

[3] Yang, M., and Tao, W.Q., Numerical Study of Natural Convection Heat Transfer in a Cylindrical Envelope with Internal Concentric Slotted Hollow Cylinder, *Numerical Heat Transfer*, Part A, vol. 22, pp. 281–305, 1992.

[4] Wang, Q.W., Natural Convection in an Inclined Cube Enclosure with Multiple Internal Isolated Plates, Ph.D. Dissertation., Xi'an Jiaotong University,China,1996.

[5] Tou, S.K.W., and Tso, C.P., 3-D Numerical Analysis of Natural Convective Liquid Cooling of 3x3 Heater Array in Rectangular Enclosure, *Int. J. Heat Mass Transfer*,vol.42, pp.3231-3244,1999.

[6] Sezai, I., and Mohamad, A.A., Natural Convection from a Discrete Heat Source on the Bottom of a Horizontal Enclosure, *Int. J. Heat Mass Transfer*, vol. 42, pp. 2257-2266, 2000.

[7] Deng, Q.H., Tang, G.F., and Li, Y.G., Interaction between Discrete Heat Source in Horizontal Natural Convection Enclosures, *Int. J. Heat Mass Transfer*, vol. 45, pp. 5117-5132, 2002.

[8] Saha, A.K., Unsteady free convection in a vertical channel with a built-in heated square cylinder, *Numerical Heat Transfer Part A*, vol. 38, no. 8, pp. 795-818, 2000.

[9] Liu, J.P., and Tao, W.Q., Numerical analysis of natural convection around a vertical channel in a rectangular enclosure. *Heat and Mass Transfer*; vol. 31, no. 5, pp. 313-321,1996.

[10] Liu, J.P., and Tao, W.Q., Bifurcation to oscillatory flow of the natural convection around a vertical channel in rectangular enclosure, *International Journal of Numerical Methods for Heat and Fluid Flow*, vol. 9, no. 2, pp. 170-85,1999.

[11] Barozzi, G.S., and Corticelli, M.A., Natural convection in cavities containing internal heat sources, *Heat and Mass Transfer*, vol. 36, pp. 473-80, 2000.

[12] Barozzi, G.S., and Corticelli, M.A., Nobile E. Numerical simulation of time-dependent buoyant flows in an enclosed vertical channel, *Heat Mass Transfer,* vol. 35, pp. 89-99, 1999.

[13] Patankar, S.V., Numerical Heat Transfer and Fluid Flow, McGraw-Hill, New York, pp. 146-152, 1980.
[14] Tao, W.Q., Numerical Heat Transfer (2ed edition) Xi'an Jiaotong University Press, pp. 244-245, 2001. (in Chinese)
[15] de Vahl Davis G., Natural Convection of Air in a Square Cavity: a Benchmark Numerical Solution, *Int . J. Meth. Fluids*, vol. 3, pp. 249-264, 1983.
[16] Kazansky, S., Dubovsky, V., Ziskind, G., and Letan, R., Chimney-Enhanced Natural Convection from a Vertical Plate: Experiments and Numerical Simulations, *Int. J. Heat Mass Transfer* ,vol. 46, pp. 497-512, 2003.
[17] Auletta, A., and Manca, O., Heat and Fluid Flow Resulting from the Chimney Effect in Symmetrically Heated Vertical Channel with Adiabatic Extensions, *Int. J. of Thermal Sciences*, vol. 41,pp. 1101-1111, 2002.
[18] Bejan, A., Convection Heat Transfer, Wiley, New York, 1984.
[19] Yang , M., Tao, W.Q. and Wang, Q.W., On the Identical Problems of Natural Convection in Enclosures and Applications of the Identity Character, *Int. J. of Thermal Sciences*, vol. 2, pp. 116–25, 1993 .